energies (given in parentheses in eV) of the interstellar atoms S (10.360), Zn (9.394), Fe (7.870), and Mg (7.646) are all larger than that typical for the larger PAH molecules (7.0), as is the case for the relative ionization energy of Si and naphthalene. In conrast, the ionization energies of Ca (6.113) and Al (5.986) are both smaller, as is the case for the relative ionization energy of Si and benzene. The ions of Ca and Al are therefore likely to form $(XPAH)^+$ adduct ions in interstellar regions of low density in the manner analogous to that observed in our laboratory for Si^+ and benzene, viz. according to reaction 26, and the reactions

$$X^+ + PAH \rightarrow X^+\cdot PAH + h\nu \quad (26)$$

of these adduct ions should mimic the behavior observed for Si^+·benzene adduct, e.g. form CaO/CaO_2 and AlO/AlO_2 from O_2 and AlOH and CaOH from H_2O. Because of the likelihood of charge transfer between the ions of the other atoms and PAH molecules, the corresponding adduct in this case must be formed by the radiative association of the neutral atom and the cation of the PAH molecule according to reaction 27. The reactions of these adduct ions should mimic those observed in this study for

$$X + PAH^+ \rightarrow X\cdot PAH^+ + h\nu \quad (27)$$

$SiC_{10}H_8^+$, reactions of the type given in (28). The capture and chemistry of atomic ions other than Si^+ will be the subject of future studies in our laboratory.

$$XPAH^+ + M \rightarrow PAH^+ + (XM) \quad (28)$$

Nothing is known about the spectroscopy of adduct ions of the type $(XPAH)^+$ so that a telescopic search for their presence in the interstellar or circumstellar gas is not yet possible. (Of course any ions, atomic or molecular, tied up in this fashion will also escape detection.) Finally we may note, by inference, that Si^+ and other atomic ions also should be captured in interstellar and circumstellar environments by PAH molecules embedded in grains of HAC and by larger hexagonal lattices such as graphite and fullerene molecules. Fullerene molecules such as C_{60} are thought to be ejected from stars into interstellar space.[23] (Alternatively the neutral atoms may be captured by the charged grains or fullerene molecules.) The chemistry which these atomic ions or atoms undergo above these surfaces with incoming molecules may well resemble that observed with small PAH molecules in the gas phase. In that case the study reported here for the chemistry of Si^+ in the presence of benzene and naphthalene should serve as an instructive prototype.

Acknowledgment. We thank the Natural Sciences and Engineering Research Council of Canada for the financial support of this research. H. Wincel is also grateful to the Polish Program CPBP-01.19 for financial support during his stay in the Ion Chemistry Laboratory at York University.

(23) Kroto, H. W. In *Polycyclic Aromatic Hydrocarbons and Astrophysics*; Leger, A., et al., Eds.; D. Reidel Publishing Co.: Dordrecht, The Netherlands, 1987; p 187.

C–H and C–C Bond Activations by Silicon. Thermochemistry and Mechanism of the Reaction of $Si^+(^2P)$ with Ethane

B. H. Boo[†] and P. B. Armentrout*[,‡]

Contribution from the Departments of Chemistry, Chungnam National University, Daejeon 305-764, Korea, and University of Utah, Salt Lake City, Utah 84112.
Received February 8, 1991

Abstract: The reaction of ground-state silicon ion with ethane (-d_0, -1,1,1-d_3, and -d_6) is investigated by using guided ion beam techniques. Absolute reaction cross sections for all product ions are determined as a function of the relative collision energy. At thermal energies, Si^+–CH_3 accounts for 90% of all products. Exothermic dehydrogenation to form $SiC_2H_4^+$ and demethanation to form $SiCH_2^+$ are observed, but these processes are inefficient. When CH_3CD_3 is employed as the reactant neutral, all products are observed to incorporate hydrogen and deuterium atoms in near-statistical distributions at low energies. This suggests that the primary HSi^+–CH_2CD_3, CH_3CD_2–SiD^+, and CH_3–Si^+–CD_3 intermediates are rapidly interconverted via a cyclic $HDSi(CH_2CD_2)^+$ intermediate.

Introduction

The reactions of atomic silicon ion with alkanes are ideal systems for examining inter- and intramolecular C–H activations by reactive silicon species as well as determining the thermochemistry of organosilicon species. Previously, we investigated the reaction of ground-state silicon ion (^2P) with methane over a broad range of kinetic energies by using guided ion beam mass spectrometry.[1] A simple reaction mechanism was able to explain the variety of endothermic processes observed. In addition, thermochemical data for SiH and $SiCH_x^+$ ($x = 1$–3) species were extracted. Here, we continue these studies by evaluating the reaction of atomic silicon ion with ethane, which has been studied once before at thermal energies only.[2] The present study provides a detailed mechanism for this reaction, additional thermochemical data for organosilicon species such as $SiCH^+$, $SiCH_3^+$, $SiC_2H_3^+$, and $SiC_2H_5^+$, and insight into the ability of silicon to activate C–H versus C–C bonds.

Experimental Section

The guided ion beam apparatus has been described in detail elsewhere.[3] Silicon ions are produced as described below. The ions are extracted, accelerated, and focused into a 60° magnetic momentum analyzer where the ^{28}Si isotope is selected. The ions are then decelerated to a desired kinetic energy and focused into an octopole ion guide. Radio-frequency electric fields in the guide create a radial potential well that traps ions over the mass range examined. The velocity of the ions parallel to the axis of the guide is unchanged. The octopole passes through a static gas cell into which a reactant neutral gas is introduced. The pressure of the reactant gas is sufficiently low ($\sim 10^{-4}$ Torr) that multiple collisions are improbable. The product and unreacted beam ions are

[†] Chungnam National University.
[‡] University of Utah. Camille and Henry Dreyfus Teacher-Scholar, 1987–1992.

(1) Boo, B. H.; Elkind, J. L.; Armentrout, P. B. *J. Am. Chem. Soc.* **1990**, *112*, 2083.
(2) Wlodek, S.; Fox, A.; Bohme, D. K. *J. Am. Chem. Soc.* **1991**, *113*, 4461.
(3) Ervin, K. M.; Armentrout, P. B. *J. Chem. Phys.* **1985**, *83*, 166.

0002-7863/91/1513-6401$02.50/0

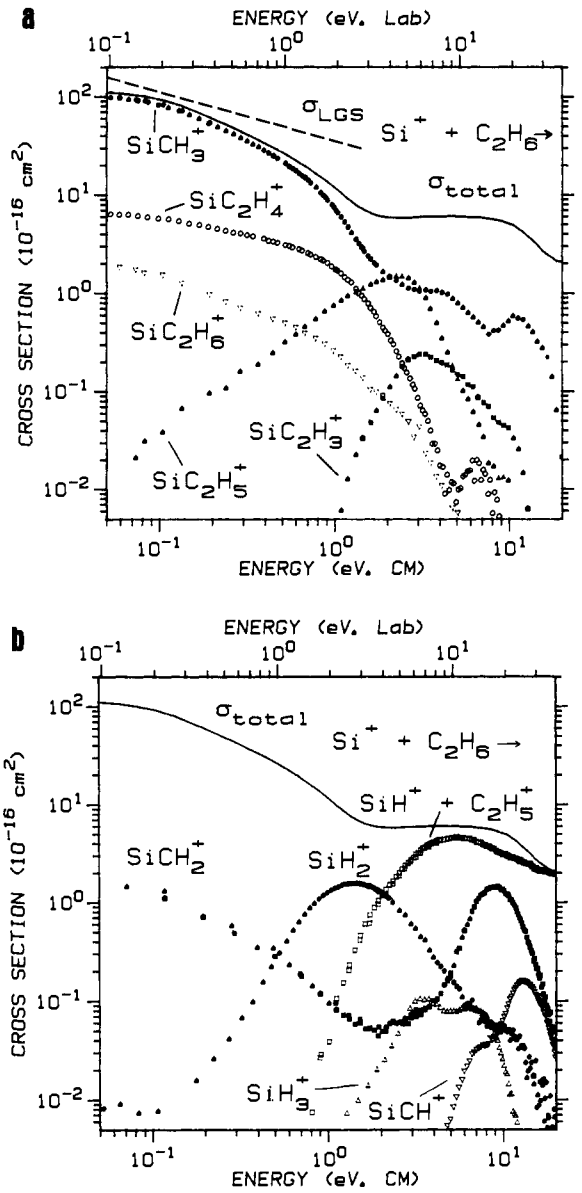

Figure 1. The variation of product cross sections for the reaction of $Si^+(^2P)$ with C_2H_6 as a function of translational energy in the laboratory frame (upper scale) and the center-of-mass energy frame (lower scale). The dashed line shows the cross section predicted by eq 23 (σ_{LGS}), and the full lines show the total reaction cross section (σ_{total}) for all products in parts a and b. The data shown were taken at an ethane pressure of 7.5×10^{-5} Torr. In part b, the open squares represent the cross section for m/z 29, the sum of SiH^+ and $C_2H_5^+$.

contained in the guide until they drift out of the gas cell. The ions are then injected into a quadrupole mass filter for product mass analysis. Finally, ions are detected with a scintillation ion detector and processed by pulse-counting techniques. Ion intensities are converted to absolute reaction cross sections as described previously.[3] Absolute and relative cross sections are estimated to have uncertainties of ±20% and ±5%, respectively.

Silicon ions are produced by surface ionization (SI).[1,4] SiH_4 is exposed to a rhenium filament resistively heated to ~2200 K where decomposition and ionization produces Si^+ but no silicon hydride ions. Since the ^4P first excited state of Si^+ is 5.46 eV higher than the ^2P ground state,[5] the SI-produced silicon ion is generated exclusively in the ground state.

Laboratory ion energies are converted to energies in the center of mass (CM) frame by using the conversion $E(CM) = E(lab)M/(m + M)$, where m and M are the masses of the projectile ion and target gas, respectively. The absolute zero of the energy scale and the distribution of ion energies are determined using the octopole as a retarding energy analyzer. This procedure is detailed elsewhere.[3] We estimate that the uncertainty in the ion energy scale is ±0.05 eV lab (±0.02 eV CM). The spread in the ion beam energy has a fwhm of 0.5 eV in the lab frame (0.27 eV CM for these experiments).

An empirical model for the kinetic energy dependence of cross sections in the threshold region of endothermic reactions is given in eq 1. Here,

$$\sigma = \sigma_0(E - E_0)^n/E^m \quad (1)$$

n and m are variable parameters, σ_0 is an energy-independent scaling factor, E is the relative translational energy, and E_0 is the threshold energy of the reaction. This form with $m = 1$ has been predicted theoretically for translationally driven reactions,[6] and previous studies have shown that this form is quite accurate for deriving reaction thresholds and describing experimental excitation functions.[1,4,7-9] Values for E_0 are determined by convoluting the model cross section with the known kinetic energy distribution of ion and neutral reactants, comparing this with the data, and then optimizing the parameters in eq 1 by using nonlinear least-squares methods.

At high energies, cross sections often reach maxima and then fall off due to product dissociation or competition with other product channels. The energy dependence of this high-energy cross-section behavior can be modeled by using a statistical assumption within the constraint of angular momentum conservation.[10] The model is controlled by two parameters: p which is an adjustable parameter, and E_D which is the energy at which the product begins decomposing.

Table I. Heats of Formation (kcal/mol) of Hydrocarbons at 298 K[a]

species	$\Delta_f H°$	species	$\Delta_f H°$
H	52.1	C_2H_2	54.5 (0.2)[b]
CH	142.0 (0.2)	C_2H_3	71.7 (0.8)[c]
CH_2	92.4 (1.0)	C_2H_4	12.5 (0.1)[b]
CH_3	34.8 (0.2)	C_2H_5	28.4 (0.5)[d]
CH_4	-17.8 (0.1)[b]	$C_2H_5^+$	217.1 (1.0)[e]
		C_2H_6	-20.0 (0.1)[b]

[a] All values except where noted are from: Chase, M. W., Jr., et al. *J. Phys. Chem. Ref. Data* **1985**, *14*, Suppl. 1 (*JANAF Tables*). This reference uses the thermal electron convention. Thus, ion heats of formation are 1.48 kcal/mol larger than values which do not include the heat of the electron. Uncertainties are in parentheses. [b] Pedley, J. B.; Naylor, R. D.; Kirby, S. P. *Thermochemical Data of Organic Compounds*; Chapman and Hall: London, 1986. [c] Ervin, K. M.; Gronert, S.; Barlow, S. E.; Gilles, M. K.; Harrison, A. G.; Bierbaum, V. M.; DePuy, C. H.; Lineberger, W. C.; and Ellison, G. B. *J. Am. Chem. Soc.* **1990**, *112*, 5750. [d] Average of values given in ref 22-26. [e] Reference 17.

Table II. Heats of Formation (kcal/mol) of Silicon Species at 298 K[a]

species	this work	literature
Si^+		297.1 (1)[b]
SiH		91.4 (1.8),[c] 90 (2)[b]
SiH^+		273.8 (1.2)[d]
SiH_2^+	275.5 (1.0)	278.0 (1.4)[d]
SiH_3^+		237.5 (1.2)[d]
$SiCH^+$	350 (3)	339 (7)[c]
$SiCH_2^+$		285 (3)[c]
$SiCH_3^+$	<242.3	235 (5)[c]
$SiC_2H_3^+$	252 (2)	>224.5 (1), <256.5 (3)[e]
$SiC_2H_4^+$	<277	
$SiC_2H_5^+$	230.3 (1.5)	
$Si(CH_3)_2^+$		211.7 (2)[f]

[a] Thermal electron convention. Thus, ion heats of formation are 1.48 kcal/mol larger than values which do not include the heat of the electron. Uncertainties are in parentheses. [b] Chase, M. W., Jr., et al. *J. Phys. Chem. Ref. Data* **1985**, *14*, Suppl. 1 (*JANAF Tables*). [c] Reference 1. [d] Value recommended in ref 4. [e] Reference 2. [f] Reference 15.

(4) Boo, B. H.; Armentrout, P. B. *J. Am. Chem. Soc.* **1987**, *109*, 3549.
(5) Moore, C. E. *Natl. Stand. Ref. Data Ser., Natl. Bur. Stand.* **1970**, *34*.
(6) Chesnavich, W. J.; Bowers, M. T. *J. Phys. Chem.* **1979**, *83*, 900.
(7) Elkind, J. L.; Armentrout, P. B. *J. Phys. Chem.* **1984**, *88*, 5454.
(8) Ervin, K. M.; Armentrout, P. B. *J. Chem. Phys.* **1986**, *84*, 6738.
(9) Armentrout, P. B. In *Structure/Reactivity and Thermochemistry of Ions*; Ausloos, P., Lias, S. G., Eds.; D. Reidel: Dordrecht, 1987; p 97.
(10) Weber, M. E.; Elkind, J. L.; Armentrout, P. B. *J. Chem. Phys.* **1986**, *84*, 1521. This paper gives E_D as $(D/f + E_0)$, where D is the ionic product dissociation energy, and f is the average fraction of product internal energy in the ionic product.

Table III. Conversions between Protiated and Deuteriated Species and between 0 K and 298 K values (kcal/mol)

species	ΔZPE[a]	$\Delta\Delta_f H°$ [b]	$\Delta_f H°_{298} - \Delta_f H°_0$
SiH	0.82[c]	−0.1	0.4
SiH^+	0.86[d]	−0.1	1.8
SiH_2^+	1.99[e]	0.2	1.1
SiH_3^+	3.71[e]	1.0	0.2
H_2	1.81[f]	0.0	
C_2H_4	7.31[f]	3.38	
C_2H_5	8.52	4.0 ± 0.4[g]	
C_2H_6	11.38[f]	5.62	

[a] Difference in zero-point energies between $A_mH_n^{(+)}$ and $A_mD_n^{(+)}$. Values are calculated using the vibrational frequencies obtained from the indicated references (ZPE$[A_mH_n^{(+)}]$ − ZPE$[A_mD_n^{(+)}]$. Values for SiD_n are calculated from these if not available directly. [b] $\Delta_f H°[A_mH_n^{(+)}] - \Delta_f H°[A_mD_n^{(+)}]$. [c] Herzberg, G.; Lagerqvist, A.; McKenzie, B. J. *Can. J. Phys.* **1969**, *47*, 1889. [d] Reference 21. [e] Pople, J. A.; Curtiss, L. A. *J. Phys. Chem.* **1987**, *91*, 155. [f] Shimanouchi, T. *Natl. Stand. Ref. Data Ser., Natl. Bur. Stand.* **1972**, *39*. [g] Derived from the heats of formation, $\Delta_f H°(C_2H_5)$ = 28.3 ± 0.4 kcal/mol, $\Delta_f H°(C_2D_5)$ = 24.3 ± 0.4 kcal/mol, given by Parmar and Benson, ref 24.

Results

The variation of the product distribution with translational energy in reaction of $^{28}Si^+$ with C_2H_6 is shown in Figure 1.[11] Similar results are also obtained for reaction with C_2D_6 and with CH_3CD_3, and verify the assignments of the various products. No other products, such as $SiCH_4^+$, were observed and thus their cross sections must be less than 10^{-18} cm^2. In the following sections, we analyze results for each individual product in detail. Thermochemistry listed for these reactions is calculated from the information in Tables I and II. Data in Table III is used to convert between different isotopic species. As discussed previously,[1] the ground states of all species with the chemical formula SiH_nC^+ should have $SiCH_n^+$ structures where all hydrogens are preferentially bound to carbon rather than silicon. Likewise, it seems reasonable that $SiH_nC_2^+$ species have the same structural preference. We assume so here unless otherwise noted.

$SiCH_3^+$. Formation of $SiCH_3^+$ is the dominant product ion in the reaction of Si^+ with ethane, Figure 1a. At low energies, formation of $SiCH_3^+$ accounts for more than 90% of the total cross section. This result is similar to that of Wlodek et al. who found that this product accounted for 80% of the thermal reactivity.[2] The reaction is clearly exothermic as evidenced by the declining cross section with increasing kinetic energy. This is consistent with the thermochemistry for reaction 2. At about 0.8 eV, the

$$Si^+ + C_2H_6 \rightarrow SiCH_3^+ + CH_3 + 0.32 \pm 0.22 \text{ eV} \quad (2)$$

cross section begins to decline more rapidly. This appears to be due to competition with other product channels since dissociation to $Si^+ + CH_3$ cannot occur until 3.9 eV. Two small cross-section features are observed at energies above ≈2 eV. Insight into the origins of these features can be obtained from isotopic labeling studies.

If reaction 2 was occurring via simple C–C bond cleavage, we would expect that the reaction of $^{28}Si^+$ with ethane-*1,1,1-d*$_3$ would lead to formation of only $SiCH_3^+$ and $SiCD_3^+$ in equal amounts. Instead, all possible silicon methyl ions are observed, Figure 2. $SiCH_3^+$ and $SiCD_3^+$ do have equal cross sections, but these are *smaller* than those for the comparably sized $SiCH_2D^+$ and $SiCHD_2^+$ cross sections. As the kinetic energy is increased, the latter species decline rapidly and exhibit neither of the high-energy cross section features mentioned above. (While the cross section labeled $SiCH_2D^+$, *m/z* 44, does show a large peak at high energies, this can be attributed to a contribution from $SiCD_2^+$.) In contrast, the $SiCH_3^+$ and $SiCD_3^+$ cross sections decline more slowly than those of $SiCH_2D^+$ and $SiCHD_2^+$, and they both show the small

(11) In some cases, the product cross sections have been corrected for overlap with adjacent products of much higher intensity. This is done only in cases where the correction is unambiguous and the resultant cross section can be verified with the isotopically labeled ethanes.

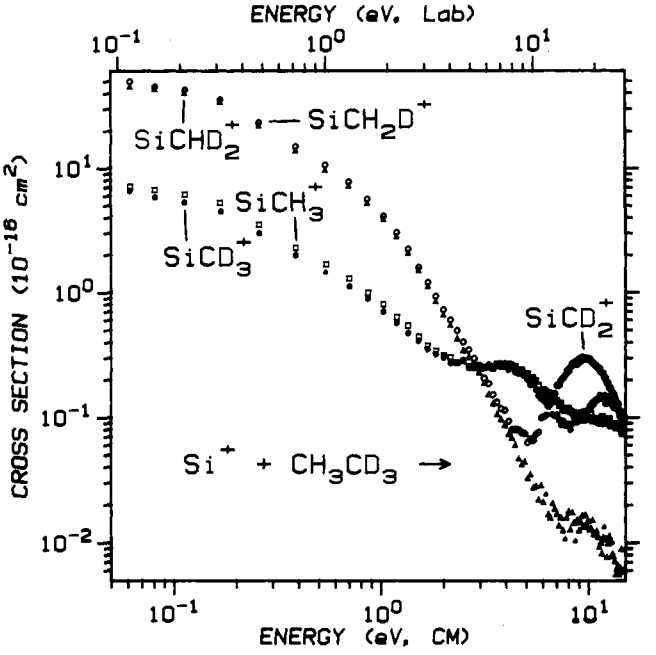

Figure 2. Cross sections for $SiCH_xD_{3-x}^+$ (x = 0, 1, 2, 3) formed in the reaction of $Si^+(^2P)$ with CH_3CD_3 as a function of the translational energy in the laboratory frame (upper scale) and the center-of-mass frame (lower scale).

feature which peaks at 4 eV, the energy at which decomposition to $Si^+ + CH_3$ (CD_3) can begin. We therefore attribute this feature to formation of these products via direct C–C bond cleavage. At the highest energies, the $SiCH_3^+$ and $SiCD_3^+$ cross sections do not match one another precisely, the latter exhibiting the second cross-section feature also visible in Figure 1a. The reasons for this difference and for this feature are not clear.

If we compare the ratios of the mixed ($SiCHD_2^+$ and $SiCH_2D^+$) and pure ($SiCH_3^+$ and $SiCD_3^+$) silicon methyl product ions (by using $SiCHD_2^+$ and $SiCH_3^+$ as representative), we find that this ratio favors the mixed isotopic species by a constant value of 6–7 up until about 1 eV. Above this energy, the ratio declines until it reaches a constant value of ~1/7 above 5 eV.

$SiC_2H_4^+$. The second most prevalent product at low kinetic energies, Figure 1a, is the result of dehydrogenation, process 3.

$$Si^+ + C_2H_6 \rightarrow SiC_2H_4^+ + H_2 \quad (3)$$

This product was also observed by Wlodek et al. at thermal energies.[2] This process declines much less rapidly with energy than the $SiCH_3^+$ cross section, suggesting that the reaction may be nearly thermoneutral or that there is a small barrier to H_2 elimination. The $SiC_2H_4^+$ cross section begins to decline near 1 eV, somewhat below the energy required for decomposition to $Si^+ + C_2H_4$, process 4. We attribute this result to competition

$$Si^+ + C_2H_6 \rightarrow Si^+ + H_2 + C_2H_4 - 1.41 \pm 0.01 \text{ eV} \quad (4)$$

with formation of other products, specifically $SiC_2H_5^+$. Indeed, the sum of the $SiC_2H_4^+$ and $SiC_2H_5^+$ cross sections forms a smooth curve, suggesting that these products are coupled via a common intermediate which decomposes preferentially to $SiC_2H_5^+$ once this channel is energetically allowed. This is reasonable since $SiC_2H_5^+$ formation from a $SiC_2H_6^+$ intermediate involves simple H atom loss (a loose transition state), while H_2 elmination to form $SiC_2H_4^+$ must involve a tight transition state.

In reaction with CH_3CD_3, Figure 3, unequivocal identification of the $SiC_2H_xD_{4-x}^+$ products is hindered due to contributions from $SiC_2H_xD_{3-x}^+$ and $SiC_2H_xD_{5-x}^+$ products having the same mass (and smaller additions from overlap of closely lying masses that are incompletely resolved in the detection mass filter). The $SiC_2HD_3^+$ (*m/z* 59) product has a sizable contribution from $SiC_2H_3D_2^+$ at higher energies, and the $SiC_2H_3D^+$ (*m/z* 57) product has a smaller contribution at high energies from

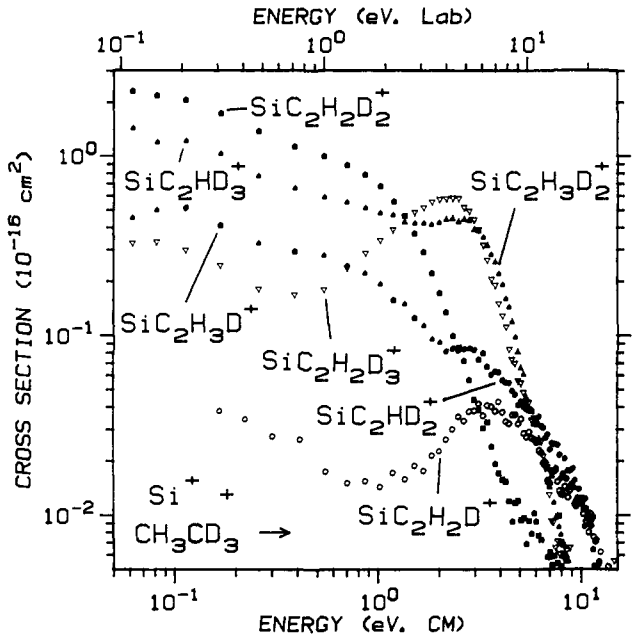

Figure 3. Cross sections for $SiC_2H_xD_y^+$ (x, y = 1, 2, 3) formed in the reaction of $Si^+(^2P)$ with CH_3CD_3 as a function of the translational energy in the laboratory frame (upper scale) and the center-of-mass frame (lower scale). The results shown are uncorrected for incomplete mass resolution; see text.

$SiC_2HD_2^+$. This can be verified by comparison with $SiC_2H_2D_3^+$ (m/z 60) and $SiC_2H_2D^+$ (m/z 56) products which have no other contributing species (but do exhibit nonzero cross sections at the lowest energies due to mass overlap with the more intense products $SiC_2HD_3^+$ (m/z 59) and $SiC_2H_3D^+$ (m/z 57), respectively), Figure 3, and by comparison with the $SiC_2H_5^+$ and $SiC_2H_3^+$ cross sections of Figure 1a.

While chemically specific cross sections are not easily derived, it is still clear that the dominant $SiC_2H_xD_{4-x}^+$ product at low kinetic energies is $SiC_2H_2D_2^+$, with appreciable contributions from formation of $SiC_2HD_3^+$ and $SiC_2H_3D^+$. The proportion of these three products is 52 ± 6, 33 ± 2, and 15 ± 4%, respectively, at the lowest energies (below 0.2 eV). These proportions change to about 57 ± 10, 27 ± 7, and 16 ± 4%, respectively, if the $SiC_2HD_3^+$ cross section is approximately corrected for the $SiC_2H_3D_2^+$ contribution. Overall, it is clear that there is substantial isotopic mixing, as in the case of the silicon methyl product ion.

$SiC_2H_6^+$. Another product formed in an exothermic process is the adduct, $SiC_2H_6^+$ (and $SiC_2H_3D_3^+$ and $SiC_2D_6^+$ in the deuteriated systems). Pressure-dependent studies (over a range of 0.07 to 0.7 mTorr) indicate that this species is formed by collisional stabilization. (These studies also verify that all other products are the result of single ion–molecule encounters.) Thus, the cross section shown in Figure 1a is for the specific ethane pressure of 7.5×10^{-5} Torr. This product was also observed by Wlodek et al. at thermal energies with a similar yield to that observed here.[2]

$SiC_2H_5^+$. Formation of $SiC_2H_5^+$ has a cross section which shows that reaction 5 is slightly endothermic, Figure 1a. This behavior

$$Si^+ + C_2H_6 \rightarrow SiC_2H_5^+ + H \quad (5)$$

is consistent with identification of this species as a silicon ethyl ion ($SiCH_2CH_3^+$), since a threshold of 0.16 ± 0.22 eV is expected assuming that $D(Si^+-C_2H_5) \approx D(Si^+-CH_3)$. Other possible structures include a silicon methyl–methylidene ion ($H_3CSiCH_2^+$) and a hydrido–ethene silicon ion complex ($HSiC_2H_4^+$).

At ~2.5 eV, the cross section falls off sharply. Of the many possible dissociation pathways for this ion, only the SiH^+ and $SiCH_3^+$ species have sufficiently large cross sections to account for the decrease in the $SiC_2H_5^+$ cross section. Overall these two decompositions are processes 6 and 7. The energetics of these

$$Si^+ + C_2H_6 \rightarrow SiH^+ + C_2H_4 + H - 2.66 \pm 0.07 \text{ eV} \quad (6)$$

$$Si^+ + C_2H_6 \rightarrow SiCH_3^+ + CH_2 + H - 4.44 \pm 0.23 \text{ eV} \quad (7)$$

processes clearly identify reaction 6 as the primary decomposition pathway, which strongly suggests that the $SiC_2H_5^+$ structure retains a C–C bond; i.e., it is unlikely to have the $H_3CSiCH_2^+$ structure. The cross section for SiH^+ shows no obvious increase at the threshold for reaction 6, but this product is probably formed primarily via a simple hydrogen abstraction reaction, discussed below.

In reaction with CH_3CD_3, the amounts of $SiC_2H_3D_2^+$ and $SiC_2H_2D_3^+$ are comparable, although there is a small preference (a factor of 1.20 ± 0.15) for the latter product (H atom loss).

$SiC_2H_3^+$. The final product shown in Figure 1a is $SiC_2H_3^+$ formed in reaction 8. This could either result from dehydroge-

$$Si^+ + C_2H_6 \rightarrow SiC_2H_3^+ + H_2 + H \quad (8)$$

nation of $SiC_2H_5^+$ or from H atom loss from $SiC_2H_4^+$. Either of these precursors has a sufficiently large cross section to account for the $SiC_2H_3^+$ cross-section magnitude; however, the sum of the $SiC_2H_3^+$ and $SiC_2H_5^+$ cross sections decreases smoothly at high energies while the sum of the $SiC_2H_3^+$ and $SiC_2H_4^+$ cross sections does not. Thus, the most likely precursor for $SiC_2H_3^+$ is the $SiC_2H_5^+$ product. This also explains the sharp maximum in the $SiC_2H_3^+$ cross section as due to the loss of the $SiC_2H_5^+$ precursor at the threshold of reaction 6.

In reaction with CH_3CD_3, the amounts of $SiC_2H_2D^+$ and $SiC_2HD_2^+$ are comparable, although there is a small preference (a factor of 1.3 ± 0.4) for the latter product. This is consistent with HD loss from the $SiC_2H_3D_2^+$ and $SiC_2H_2D_3^+$ parent ions.

SiH_2^+. Figure 1b shows that the formation of SiH_2^+ is a major product at intermediate kinetic energies. This ion must be formed in reaction 9 and is in direct competition with reaction 3. The

$$Si^+ + C_2H_6 \rightarrow SiH_2^+ + C_2H_4 - 0.58 \pm 0.08 \text{ eV} \quad (9)$$

SiH_2^+ cross section is observed to decline beginning about 1.4 eV, Figure 1b. This is in agreement with the calculated endothermicity for dissociation to $Si^+ + H_2$, overall reaction 4, and is clearly below the energy required for decomposition to $SiH^+ + H$, overall reaction 6.

In reaction with CH_3CD_3, the dominant product is $SiHD^+$, but appreciable amounts of SiH_2^+ and SiD_2^+ are also formed. The relative amounts of these three products are about 58 ± 4, 29 ± 3, and 13 ± 2%, respectively, although the precise values may differ slightly due to some mass overlap. Note that these proportions match those for $SiC_2H_2D_2^+$, $SiC_2HD_3^+$, and $SiC_2H_3D^+$, respectively.

SiH^+, $C_2H_5^+$. The largest product ion at high kinetic energies has m/z 29, Figure 1b. This could be $^{28}SiH^+$ or $C_2H_5^+$. The former can be generated via the hydrogen atom transfer reaction, process 10, while the latter corresponds to the hydride transfer

$$Si^+ + C_2H_6 \rightarrow SiH^+ + C_2H_5 - 1.09 \pm 0.08 \text{ eV} \quad (10)$$

process, reaction 11.

$$Si^+ + C_2H_6 \rightarrow SiH + C_2H_5^+ - 1.36 \pm 0.10 \text{ eV} \quad (11)$$

To separate these processes, we can employ completely deuteriated ethane to characterize processes 12 and 13, the deuterium

$$Si^+ + C_2D_6 \rightarrow SiD^+ + C_2D_5 - 1.16 \pm 0.08 \text{ eV} \quad (12)$$

$$Si^+ + C_2D_6 \rightarrow SiD + C_2D_5^+ - 1.44 \pm 0.10 \text{ eV} \quad (13)$$

analogues of reactions 10 and 11. These data are shown in Figure 4. (The latter mass channel has a small contribution from process 14, but this is less than 20% of the total based on the magnitude

$$Si^+ + C_2D_6 \rightarrow SiD_3^+ + C_2D_3 \quad (14)$$

of the SiH_3^+ cross section shown in Figures 1b and 4.) Figure 4 also shows that the experimental cross section for m/z 29 in the C_2H_6 system is similar to the sum of the cross sections for reactions 12 and 13. The general behavior of the SiH^+ cross section has also been verified by examining reaction 15.

$$^{30}Si^+ + C_2H_6 \rightarrow {}^{30}SiH^+ + C_2H_5 - 1.09 \pm 0.08\text{eV} \quad (15)$$

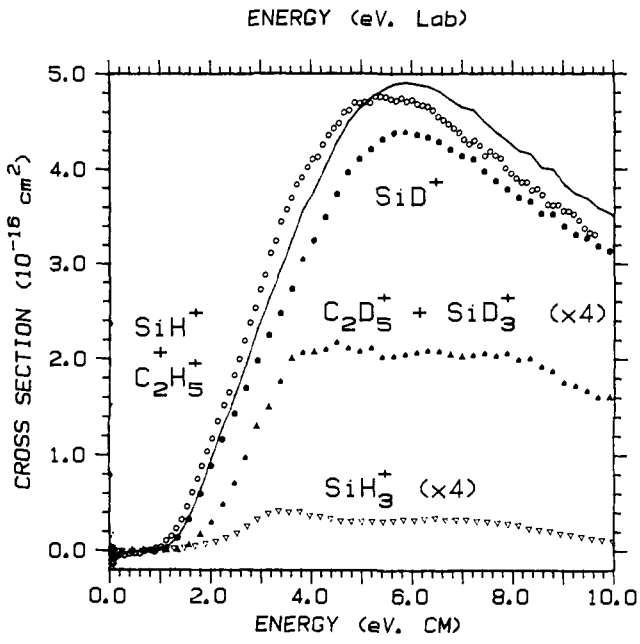

Figure 4. Cross sections for reactions 12 (closed circles), 13 (closed triangles, multiplied by 4), 22 (open triangles, multiplied by 4), and the sum of reactions 10 and 11 (open circles) as a function of the translational energy in the laboratory frame (upper scale) and the center-of-mass frame (lower scale). The line shows the sum of the cross sections for SiD^+, $C_2D_5^+$ and SiD_3^+.

As shown in Figures 1b and 4, the cross section for SiH^+ begins to decline at ~5 eV. This is presumably due to product dissociation, process 16. Since the observed onset for this process is

$$Si^+ + C_2H_6 \rightarrow Si^+ + H + C_2H_5 - 4.36 \pm 0.02 \text{ eV} \quad (16)$$

somewhat higher than the thermodynamic limit, this indicates that the C_2H_5 neutral product must carry away some fraction of the total available energy in internal degrees of freedom.

$SiCH_2^+$. The cross section for $SiCH_2^+$ is shown in Figure 1b. It is possible that the cross section at low energies may be too large due to overlap with the much more intense $SiCH_3^+$ product signal, although the results shown were reproducible and results for C_2D_6 as the reactant neutral, where the possibility of mass overlap is negligibly small, yield a quantitatively similar result. The size of the $SiCH_2^+$ cross section at low energies is quite small, accounting for about 1.5% of the product yield at our lowest energies. This result differs appreciably from the observations of Wlodek et al. who report 15% $SiCH_2^+$ at thermal energies.[2] It is possible that this is the result of a multiple reaction sequence in this flow tube experiment.

The inefficient reactivity observed at low energies must be due to the near-thermoneutral process 17. At higher energies, the

$$Si^+ + C_2H_6 \rightarrow SiCH_2^+ + CH_4 + 0.43 \pm 0.14 \text{ eV} \quad (17)$$

cross section increases substantially beginning about 3 to 4 eV. This must be due to process 18, which corresponds to dissociation

$$Si^+ + C_2H_6 \rightarrow SiCH_2^+ + H + CH_3 - 4.11 \pm 0.14 \text{ eV} \quad (18)$$

of the major product $SiCH_3^+$. Since the second feature is larger than the low-energy one, the molecular elimination of CH_4 from $SiC_2H_6^+$ is clearly much less efficient than hydrogen atom elimination from $SiCH_3^+$. This is presumably because reaction 18 proceeds via a simple bond fission, while process 17 involves a tight transition state.

At still higher energies, the cross section falls off beginning about 9 eV. The product dissociation channels, processes 19 and

$$Si^+ + C_2H_6 \rightarrow Si^+ + CH_2 + H + CH_3 - 8.64 \pm 0.05 \text{ eV} \quad (19)$$

20, can probably explain this observation. Since $SiCH^+$ is only

$$Si^+ + C_2H_6 \rightarrow SiCH^+ + 2H + CH_3 - 8.71 \pm 0.31 \text{ eV} \quad (20)$$

a minor product at these energies, reaction 19 must be the dominant decomposition channel, although it cannot be observed directly since the product and reactant ions are the same.

In reaction with CH_3CD_3, the $SiCH_xD_{2-x}^+$ products cannot be measured at low energies since they have the same mass as several of the $SiCH_xD_{3-x}^+$ products. For the high-energy feature, $SiCH_2^+$ and $SiCD_2^+$ are the dominant products. Little if any $SiCHD^+$ is generated. (Some ambiguity arises because $SiCH_3^+$ has the same mass as this product. We observe that the cross section for m/z 43 declines monotonically with no noticeable increase over the energy range where the high-energy features in $SiCH_2^+$ and $SiCD_2^+$ are observed.) This is further evidence that, above ~4 eV, the $SiCH_xD_{2-x}^+$ species are generated by H or D atom loss from $SiCH_3^+$ and $SiCD_3^+$, the dominant silicon methyl product ions at elevated kinetic energies.

$SiCH^+$. The high-energy feature in the cross section for $SiCH^+$, Figure 1b, can be accounted for by reaction 20. Process 21 can

$$Si^+ + C_2H_6 \rightarrow SiCH^+ + H_2 + CH_3 - 4.19 \pm 0.31 \text{ eV} \quad (21)$$

account for the low-energy feature. This is probably a minor decomposition pathway for the $SiCH_3^+$ product. Since the second feature is much larger than the low-energy one, the molecular elimination of H_2 from $SiCH_3^+$, process 21, appears to be much less efficient than hydrogen atom elimination from $SiCH_2^+$, reaction 20. This is presumably because reaction 20 proceeds via simple bond fission while process 21 involves a tight transition state.

SiH_3^+. The only other product observed in the ethane system is SiH_3^+, Figure 1b, which must be formed in process 22. This

$$Si^+ + C_2H_6 \rightarrow SiH_3^+ + C_2H_3 - 1.39 \pm 0.08 \text{ eV} \quad (22)$$

product has a very small cross section that barely exceeds 10^{-17} cm^2 but rises from an energy near the expected thermodynamic limit. The observation of this product clearly indicates that the mobility of the hydrogen atoms is fairly high in this system.

Discussion

Reaction Efficiency. As shown in Figure 1a, the overall reaction of Si^+ with ethane is very efficient at thermal energies, a result quite different from the $Si^+ + CH_4$ system where no reaction occurs at thermal energies.[1] We can compare the total absolute cross section with the collision cross section predicted for ion-induced dipole interactions, as given by the Langevin–Gioumousis–Stevenson (LGS) cross section,[12] eq 23 (where α refers to

$$\sigma_{LGS}(E) = \pi e(2\alpha/E)^{1/2} \quad (23)$$

the polarizability of ethane, 4.39 Å^3).[13] We find that our results for both C_2H_6 and C_2D_6 are about 78% of σ_{LGS} at the lowest energies. Converted to a rate constant,[14] this is equivalent to a 298 K rate constant of $(1.0 \pm 0.2) \times 10^{-9}$ cm^3/s for both ethane, d_0 and d_6 compared to $k_{LGS} = 1.3 \times 10^{-9}$ cm^3/s. This result is in good agreement with the rate constant of $(0.8 \pm 0.24) \times 10^{-9}$ cm^3/s measured by Bohme and co-workers for reaction of Si^+ with C_2H_6 at 296 K.[2]

Reaction Mechanism. The mechanism to be discussed is based on thermochemical arguments, reaction efficiencies, and labeling experiments. The arguments which follow can be used to construct the semiquantitative potential energy surface shown in Figure 5. The energies of the reactant and product channels are calculated from the information given in Tables I and II. Energies of the intermediates are estimated as detailed below.

As previously discussed for reaction of $Si^+(^2P)$ with methane,[1] the initial step in the reaction of Si^+ with ethane must involve

(12) Gioumousis, G.; Stevenson, D. P. *J. Chem. Phys.* **1958**, *29*, 294.
(13) Rothe, E. W.; Bernstein, R. B. *J. Chem. Phys.* **1959**, *31*, 1619.
(14) Reaction cross sections are converted to rate constants as described in ref 3. This is approximately given by $k(\langle E \rangle) = \sigma(E)\cdot(2E/\mu)^{1/2}$ where $\langle E \rangle = E + 3\gamma kT/2$. The parameters μ and γ are defined as $\mu = mM/(m + M)$ and $\gamma = m/(m + M)$, where m and M are the masses of the ionic and neutral reactants, respectively.

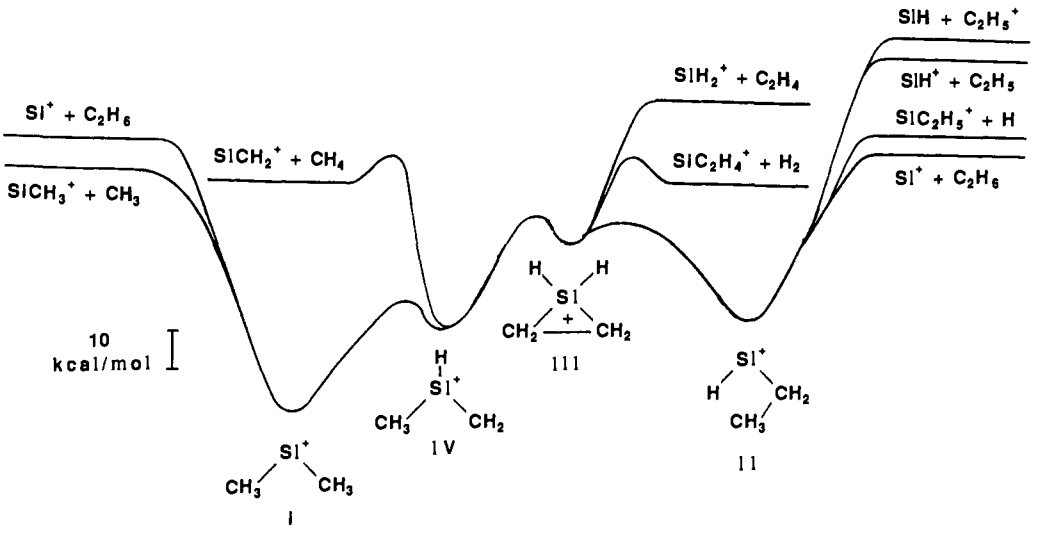

Figure 5. Semiquantitative potential energy surface for the reaction of Si^+ with C_2H_6.

insertion into the covalent bonds of the hydrocarbon. Such insertions of silicon ion into either the C–H or C–C bonds of ethane are both energetically feasible. Insertion into the C–C bond is exothermic by 65 kcal/mol, a value calculated with the thermodynamic data given in Tables I and II. The resulting $CH_3SiCH_3^+$ intermediate I could then undergo a Si–CH_3 bond cleavage to yield the dominant $SiCH_3^+$ product, Figure 5.

Intermediate I does not lead directly to the other major low-energy products: $SiC_2H_4^+$, $SiC_2H_5^+$, SiH_2^+, and SiH^+. These can be explained easily by a C–H bond insertion step. This too is exothermic, by an estimated 42 kcal/mol (assuming that the Si^+–ethyl bond energy in the H–Si^+–C_2H_5 intermediate, II, is comparable to the Si^+–methyl bond energy of H–Si^+–CH_3, 67 kcal/mol[15]). This intermediate can lead directly to the $SiC_2H_5^+$, SiH^+, and $C_2H_5^+$ products by bond fission at high energies, Figure 5. At low energies, intermediate II could rearrange to $H_2Si(C_2H_4)^+$, III.[16,17] This formula can either represent a dihydride ethene silicon ion complex or the silacyclopropane ion. In all likelihood, these forms are basically equivalent to one another. Intermediate III can now reductively eliminate H_2 to yield $SiC_2H_4^+$ or it can eliminate ethene to form SiH_2^+, Figure 5. We anticipate that the former reaction may have a reverse activation barrier, while the thermochemistry discussed below shows that that latter reaction does not.

If this reaction scheme were complete, then the major product ion in reaction with CH_3CD_3 would be $SiCH_3^+$ and $SiCD_3^+$. The observation that $SiCH_2D^+$ and $SiCHD_2^+$ are the major species observed at low kinetic energies requires a more complex mechanism. In considering the various possibilities, we restrict the formation of these species to processes which generate the silicon–methyl ion, rather than a H—Si^+=CH_2 structure. As discussed previously,[1] this latter isomer is calculated to be 48 kcal/mol higher in energy,[18] meaning that its formation from $Si^+ + C_2H_6$ is endothermic by 1.76 eV. It is possible, however, that such an isomer could explain some of the high-energy features observed in the $SiCH_3^+$ cross section.

Further insight into these products comes from the observation that there is near-statistical hydrogen scrambling in all products. The $SiCH_2D^+$ and $SiCHD_2^+$ products are observed to be about six to seven times more intense than the $SiCH_3^+$ and $SiCD_3^+$ products, while a purely statistical distribution predicts a factor of 9. The small difference in the ratio is probably because the bond cleavages of the primary intermediates can lead only to $SiCH_3^+$ and $SiCD_3^+$, while $SiCH_2D^+$ and $SiCHD_2^+$ require rearrangement. For SiH_2^+, $SiHD^+$, and SiD_2^+, the observed distribution is 29:58:13%, respectively. The $SiC_2HD_3^+$, $SiC_2H_2D_2^+$, and $SiC_2H_3D^+$ products, which compete directly with the silicon dihydride ion products, exhibit a similar distribution of 27:57:16%, respectively. The statistical distribution is 20:60:20% and is identical for both $SiH_xD_{2-x}^+$ and $SiC_2H_xD_{4-x}^+$.

These observations demonstrate that hydrogen randomization is very facile (as it was in the case of the reaction of Si^+ with SiH_4),[4] which can be accommodated if the intermediates are all much lower in energy than the reactants and all products, Figure 5. One reasonable mechanism for hydrogen scrambling in the case of the $SiH_xD_{2-x}^+$ and $SiC_2H_xD_{4-x}^+$ products involves intermediates II and III. Reversible hydrogen and deuterium atom migration allows an efficient route to complete isotopic randomization. Some preference for H atom transfer could explain the predominance of SiH_2^+ and $SiC_2HD_3^+$ products over SiD_2^+ and $SiC_2H_3D^+$ species.

This mechanism does not yet explain the observation of the $SiCH_2D^+$ and $SiCHD_2^+$ products. One possible route for the formation of these species is that intermediate I can interconvert with II, where scrambling occurs as described above. This conversion presumably requires generation of $CH_3(H)SiCH_2^+$, intermediate IV,[19] which can be formed from I by a hydrogen transfer from C to Si, from II by a methyl migration from C to Si, or from III by C–C bond cleavage and hydrogen transfer (a step which is analogous to the conversion of III to II). Of course, if I and II can easily interconvert, then direct insertion into *both* C–H and C–C bonds is not necessary. Hence, we can make no assignments regarding the relative ability of silicon to activate C–H versus C–C bonds. An alternate mechanism avoids production of intermediate I altogether. Now, II decomposes directly to $SiCH_3^+ + CH_3$ via C–C bond cleavage accompanied by a concerted H-atom shift from Si to C in order to generate the ground-state silicon methyl ion. Such a constrained mechanism seems unlikely to produce the $SiCH_3^+$ product with the high efficiencies observed.

The situation can change as the energy increases since dissociation of the primary intermediates will begin to occur more rapidly until these processes become faster than the rate of con-

(15) Shin, S. K.; Corderman, R. R.; Beauchamp, J. L. *Int. J. Mass Spectrom. Ion Processes*, **1990**, *101*, 257.

(16) The energy of this intermediate is estimated in two ways. (1) The bond energy of H_2Si^+–C_2H_4 is assumed equal to that for Si^+–C_2H_4, ≥33 kcal/mol, which gives $\Delta_f H(H_2SiC_2H_4^+) \leq 258$ kcal/mol. (2) Comparison of $C_3H_8^+$ ($\Delta_f H$ = 229 kcal/mol)[17] and c-$C_3H_6^+$ ($\Delta_f H$ = 241.5 kcal/mol)[17] with $H_2Si(CH_3)_2^+$ ($\Delta_f H$ = 216 kcal/mol)[15] suggests that $\Delta_f H[H_2Si(CH_2)_2^+] \approx 254$ kcal/mol.

(17) Lias, S. G.; Bartmess, J. E.; Liebman, J. F.; Holmes, J. L.; Levin, R. D.; Mallard, W. G. *J. Phys. Chem. Ref. Data* **1988**, *17*, Suppl. 1 (GIANT Tables).

(18) Ragavachari, K. Personal communication.

(19) The heat of formation of this intermediate is estimated as 230 kcal/mol by assuming that the $CH_3(H)Si^+$–CH_2 bond energy is similar to that for $CH_3(H)Si^+$–CH_3, 102 kcal/mol.[15]

Table IV. Values of n, E_0, p, and E_D Used To Model Excitation Functions

system	product	n	E_0 (eV)[a]	p	E_D (eV)
$Si^+ + C_2H_6$	SiH^+	1.7	1.06 (0.06)	1	4.52
	SiH_2^+	1.2	0.41 (0.05)	1	1.45
	SiH_3^+	2.5	0.65 (0.05)		
	$SiCH^+$	1.0	4.66 (0.1)	2	9.2
	$SiCH_2^+$	1.0	1.04 (0.1)		
	$SiCH_3^+$		<0		
	$SiC_2H_3^+$	1.7	1.16 (0.1)	1	5.27
	$SiC_2H_4^+$		<0		
	$SiC_2H_5^+$	1.7	0.23 (0.04)	4	2.55
	$SiC_2H_6^+$		<0		
$Si^+ + C_2D_6$	SiD^+	1.7	1.16 (0.04)	1	5.27
	$C_2D_5^+$	1.7	1.66 (0.1)		
	SiD_2^+	1.2	0.62 (0.03)	1	1.70
	$SiCD^+$	1.0	5.40 (0.1)		
	$SiCD_2^+$	1.0	1.40 (0.1)	1	4.62
	$SiCD_3^+$		<0		
	$SiC_2D_3^+$	1.5	1.41 (0.04)	1	3.75
	$SiC_2D_4^+$		<0		
	$SiC_2D_5^+$	1.7	0.40 (0.05)	4	3.15
	$SiC_6D_6^+$		<0		

[a] Numbers in parentheses are the error associated with the value.

version between the primary intermediates. This is clearly demonstrated in Figure 2. At elevated energies, the cross sections for $SiCH_3^+$ and $SiCD_3^+$ become much larger than those for $SiCH_2D^+$ and $SiCHD_2^+$. This is presumably due to prompt dissociation from intermediate I.

The remaining product observed is $SiCH_2^+$. At low energies, this is accompanied by CH_4. This process could occur by a four-center elimination of methane from intermediates I or II, or reductive elimination of CH_4 from the silicon center in IV, Figure 5. At high energies, $SiCH_2^+$ is formed by H-atom loss from $SiCH_3^+$.

Thermochemistry

The threshold regions of the various cross sections are analyzed by using eq 1 with $m = 1$. This model cross section nicely reproduces the experimental cross sections observed in the ethane system. The optimized parameters used for each reaction are given in Table IV.

C_2H_5. The threshold of process 10, $E_0 = 1.06 \pm 0.06$ (seven data sets), provides a heat of formation for the $SiH^+ + C_2H_5$ products of 301.5 ± 1.7 kcal/mol. The heat of formation of SiH^+ is now firmly established by both spectroscopic[20,21] and previous measurements in our laboratory[1,4,7] as 273.8 ± 1.2 kcal/mol. We therefore use this value to derive the heat of formation of the ethyl radical. We obtain $\Delta_f H°(C_2H_5) = 27.7 \pm 2.1$ kcal/mol. In the reaction with C_2D_6, the threshold for reaction 12 yields $\Delta_f H°(C_2D_5) = 24.3 \pm 1.8$ kcal/mol, which can be converted to $\Delta_f H°(C_2H_5) = 28.3 \pm 1.9$ kcal/mol, Table III. The average of the two values, 28.0 ± 1.4 kcal/mol, is in excellent agreement with several recent determinations of this value, 28.36 ± 0.4,[22] 28.3 ± 1.1,[23] 28.3 ± 0.4,[24] 28.7 ± 0.7,[25] and 28.4 ± 0.5,[26] but exceeds the older value taken from halogenation studies, 25.9 ± 1.0 kcal/mol.[27]

$C_2H_5^+$. The threshold of reaction 13, $E_0 = 1.66 \pm 0.1$ eV, is somewhat above that calculated from the literature thermochemistry, 1.44 ± 0.10 eV. (This value assumes that the difference in the heats of formation of $C_2H_5^+$ and $C_2D_5^+$ is similar to the difference between the neutral counterparts, Table III.) The threshold for reaction 13 may be shifted to higher energies as a result of competition with reaction 12 and because C_2H_5 is not easily ionized at threshold due to poor Franck–Condon overlap. Indeed, the effective ionization energy of C_2D_5 that can be obtained from our measured threshold for reaction 13 is 8.35 eV, in good agreement with the onset for C_2H_5 ionization as measured by photoelectron spectroscopy, 8.39 eV.[28]

SiH_2^+. The threshold of reaction 9 is obtained as 0.41 ± 0.05 eV, which provides a heat of formation, $\Delta_f H°(SiH_2^+) = 274.1 \pm 1.5$ kcal/mol. The deuterium analogue yields a heat of formation, $\Delta_f H°(SiD_2^+) = 276.7 \pm 1.2$ kcal/mol which is converted to 276.9 ± 1.2 kcal/mol for $\Delta_f H°(SiH_2^+)$ by using Table III. The average of the two values is 275.5 ± 1.0 kcal/mol. This is in good agreement with an average value derived previously in our laboratories (which included a preliminary value for this experiment), 276.1 ± 1.7 kcal/mol.[4] It is also close to several photoionization values, 278.8,[29] 275.4,[30] and 277.7 kcal/mol,[20] and our recommended value of 278.0 ± 1.4 kcal/mol.[4]

$SiCH^+$. A $\Delta_f H°(SiCH^+)$ value of 350 ± 3 kcal/mol is derived from the threshold of reaction 21 given in Table IV. This is near our previously reported value of 339 ± 7 kcal/mol.[1]

$SiCH_2^+$. As noted previously by Wlodek et al.,[2] the observation of reaction 17 at thermal energies implies that $\Delta_f H°(SiCH_2^+) < 295 \pm 1$ kcal/mol. This is in agreement with our previously determined heat of formation $\Delta_f H°(SiCH_2^+) = 285 \pm 3$ kcal/mol.[1]

$SiCH_3^+$. Formation of this product ion is observed to be exothermic, indicating that the Si^+–CH_3 bond is stronger than the CH_3–CH_3 bond. This yields an upper limit of 242.3 kcal/mol for the heat of formation of $SiCH_3^+$, in line with the thermochemistry of 235 ± 5 kcal/mol determined previously.[1]

$SiC_2H_3^+$. A threshold of $E_0 = 1.16 \pm 0.1$ eV for reaction 8 provides a heat of formation of $SiC_2H_3^+$ of 252 ± 3 kcal/mol. Results for the C_2D_6 system yield a comparable value, $\Delta_f H°(SiC_2D_3^+) = 251 \pm 2$ kcal/mol. These values are consistent with the limits established by Wlodek et al. of 224.5 ± 1 kcal/mol < $\Delta_f H°(SiC_2H_3^+) < 256.5 \pm 3$ kcal/mol.[2] Our value for the heat of formation leads to a Si^+–C_2H_3 bond energy of 117 ± 3 kcal/mol, which is somewhat stronger than $D(Si^+–CH_3) = 97 \pm 5$ kcal/mol. This is probably consistent with a silicon ion–vinyl structure for the $SiC_2H_3^+$ species, with additional stabilization of the silicon cation by the CC π electrons.

$SiC_2H_4^+$. The observation that reaction 3 is exothermic or near thermoneutral places the heat of formation of $SiC_2H_4^+$ at ≤277 kcal/mol. If the ground-state structure of $SiC_2H_4^+$ is Si^+–ethene, then this implies a Si^+–ethene bond energy of ≥33 kcal/mol. However, an alternate structure is the silicon ethylidene ion, $Si^+{=}CH{-}CH_3$. Given $\Delta_f H°(CHCH_3) = 88.5$ kcal/mol,[31] this assumption yields a bond energy, $D°(Si^+{=}CHCH_3) \geq 108.5$ kcal/mol, which is reasonably consistent with $D°(Si^+{=}CH_2) = 104 \pm 3$ kcal/mol.[1] Unfortunately, no structural information can be gained from the isotope labeling studies since statistical distributions of the various products are obtained.

$SiC_2H_5^+$. The heat of formation for this ion is derived to be 230.3 ± 1.5 kcal/mol from the measured threshold of process 5. Results for the C_2D_6 system yield a comparable value of 227.7

(20) Berkowitz, J.; Greene, J. P.; Cho, H.; Ruscic, B. *J. Chem. Phys.* **1987**, *86*, 1235. All values in this paper are at 0 K. Citations here have been corrected to 298 K using Table III.

(21) (a) Carlson, T. A.; Copley, J.; Duric, N.; Elander, N.; Erman, P.; Larsson, M.; Lyyra, M. *Astron. Astrophys.* **1980**, *83*, 238. (b) Douglas, A. E.; Lutz, B. L. *Can. J. Phys.* **1970**, *48*, 247.

(22) Brouard, M.; Lightfoot, P. D.; Pilling, M. J. *J. Phys. Chem.* **1986**, *90*, 445.

(23) Doering, W. v. E. *Proc. Natl. Acad. Sci. U.S.A.* **1981**, *78*, 5279.

(24) Parmar, S. S.; Benson, S. W. *J. Am. Chem. Soc.* **1989**, *111*, 57.

(25) Russell, J. J.; Seetula, J. A.; Gutman, D. *J. Am. Chem. Soc.* **1988**, *110*, 3092.

(26) Pacey, P. D.; Wimalasena, J. H. *J. Phys. Chem.* **1984**, *88*, 5657.

(27) McMillen, D. G.; Golden, D. M. *Annu. Rev. Phys. Chem.* **1982**, *33*, 493.

(28) Houle, F. A.; Beauchamp, J. L. *J. Am. Chem. Soc.* **1979**, *101*, 4067.

(29) Ding, A.; Cassidy, R. A.; Cordis, L. S.; Lampe, F. W. *J. Chem. Phys.* **1985**, *83*, 3426. Note that these authors use the stationary electron convention and $\Delta_f H°(SiH_4) = 7.3$ kcal/mol. The values cited here have been corrected for these differences.

(30) Reference 15 cites a stationary electron convention value of $\Delta_f H°(SiH_2^+) = 273.9 \pm 0.7$ kcal/mol.

(31) Frenking, G.; Schmidt, J. *Tetrahedron*, **1984**, *40*, 2123.

± 1.5 kcal/mol for the perdeuteriated species. The former value yields a $Si^+-C_2H_5$ bond energy of 95 ± 2 kcal/mol, which is very close to $D°(Si^+-CH_3)$ = 97 ± 5 kcal/mol.[1] This is consistent with a silicon ion-ethyl structure for this species. The alternate $H-Si^+-C_2H_4$ structure can be further discounted by evaluating the bond energy, $D°(SiC_2H_4^+-H) \leq 99$ kcal/mol. This is much closer to a C-H bond strength than to the Si^+-H bond strength of 75.4 ± 0.9 kcal/mol, although this conclusion is questionable if reaction 3 is very exothermic rather than being thermoneutral.

Acknowledgment. This work was supported by a grant from the National Science Foundation (Grant No. CHE-8917980) and by the Air Force Wright Aeronautical Laboratories. One of the authors (B.H.B.) is grateful to the Korea Science and Engineering Foundation for the partial financial support. We also thank D. K. Bohme for communication of results prior to publication.

van der Waals Complexes of Chemically Reactive Gases: Ozone-Acetylene

J. Z. Gillies,[†] C. W. Gillies,*[,‡] F. J. Lovas,[§] K. Matsumura,[§,⊥] R. D. Suenram,[§] E. Kraka,[∥] and D. Cremer[∥]

Contribution from the Department of Chemistry, Siena College, Loudonville, New York 12211, Department of Chemistry, Rensselaer Polytechnic Institute, Troy, New York 12180, Molecular Physics Division, National Institute of Standards and Technology, Gaithersburg, Maryland 20899, and Theoretical Chemistry, University of Göteborg, Kemigarden 3, S-41296 Göteborg, Sweden. *Received February 12, 1991*

Abstract: A pulsed-beam Fabry-Perot cavity Fourier-transform microwave spectrometer was used to observe rotational spectra of the normal, d_1- and d_2-isotopic species of the ozone-acetylene van der Waals complex. The work employed a modified, pulsed-solenoid valve which served as a flow reactor to sample the reacting gas mixture of 1% ozone and 1% acetylene in argon. The *c*-type transitions of the three isotopic species were split into tunneling doublets due to an internal rotation of acetylene which exchanges the hydrogen (deuterium) atoms. Spectral constants of the two tunneling states for each isotopic species were obtained independently from fits to an asymmetric top Watson Hamiltonian. Stark effect measurements for $O_3-C_2H_2$ gave μ_a = 0.041 (1) and μ_c = 0.473 (1) D. The microwave data show the complex has C_s symmetry with the molecular axis of acetylene located parallel to the OOO plane of ozone at a center-of-mass separation of R_{cm} = 3.251 (2) Å. Ab initio calculations at the MP4(SDQ)/6-31G(d,p) level have found the terminal oxygens of ozone are tilted symmetrically toward the molecular axis of acetylene. The combined microwave and ab initio results indicate that the interaction potential surface of ozone plus acetylene is quite similar to ozone plus ethylene at van der Waals distances.

I. Introduction

Molecular-beam-electric-resonance and pulsed-nozzle Fourier-transform microwave spectroscopies have been used to characterize a large number of van der Waals complexes. The microwave measurements determine the geometries and provide data which can be related to the internal motions of the complexes.[1-3] Generally, these techniques have been applied to the study of weakly bound complexes composed of monomer subunits which do not chemically react with one another. Recently we reported the formation of a van der Waals complex between ozone and ethylene, $O_3-C_2H_4$.[4] In this case, the two monomers are quite reactive with a gas-phase bimolecular rate constant of 1.02×10^6 cm^3 mol^{-1} s^{-1} at room temperature.[5] The $O_3-C_2H_4$ complex was formed in the supersonic expansion obtained from a pulsed-beam valve which was modified so that it sampled a reacting mixture of ozone and ethylene diluted in argon. It was detected in the Fabry-Perot cavity of a Fourier-transform microwave spectrometer.

Since the $O_3-C_2H_4$ complex is located on the reaction potential surface of ozone plus ethylene, the work provided the geometry of a chemical species at large distances along the reaction coordinate. A combination of microwave results and ab initio calculations finds the van der Waals complex has an envelope conformation with C_s symmetry.[6] Ozone plus ethylene is a classical example of a 1,3-dipolar cycloaddition reaction which is thermally allowed by Woodward-Hoffman symmetry rules.[7-10] In the gas phase and solution, the first step in the reaction is concerted and leads to the cycloaddition product 1,2,3-trioxolane ($\overline{CH_2OOO-CH_2}$).[7,8,11] Microwave studies have shown that 1,2,3-trioxolane has a similar oxygen envelope conformation with C_s symmetry[11] as found for the $O_3-C_2H_4$ weakly bound complex.[4,6] Ab initio calculations indicate that the transition-state geometry corresponds to the oxygen envelope conformation.[12] Furthermore, they suggest

[†] Siena College.
[‡] Rensselaer Polytechnic Institute.
[§] National Institute of Standards and Technology.
[⊥] Permanent Address: Seinan Gakuin University, Nishijin, Sawaraku, Fukuoka 814, Japan.
[∥] University of Göteborg.

(1) Dyke, T. R. *Top. Curr. Chem.* **1984**, *120*, 86.
(2) Legon, A. C.; Millen, D. J. *Chem. Rev.* **1986**, *86*, 635.
(3) Novick, S. E. Bibliography of Rotational Spectra of Weakly Bound Complexes. In *Structure and Dynamics of Weakly Bound Molecular Complexes*: Weber, A., Ed.; Reidel Publishing Co.: Dordrecht, Holland, 1987.
(4) Gillies, J. Z.; Gillies, C. W.; Suenram, R. D.; Lovas, F. J.; Stahl, W. *J. Am. Chem. Soc.* **1989**, *111*, 3073.
(5) Herron, J. T.; Huie, R. E. *J. Phys. Chem.* **1974**, *78*, 2085 and references therein.
(6) Gillies, C. W.; Gillies, J. Z.; Suenram, R. D.; Lovas, F. J.; Kraka, E.; Cremer, D. *J. Am. Chem. Soc.* **1991**, *113*, 2412.
(7) Bailey, P. S. *Ozonation in Organic Chemistry*; Academic Press: New York, 1978; Vol. 1; 1982, Vol. 2
(8) Kuczkowski, R. L. *1,3-Dipolar Cycloadditions*; Padwa, A., Ed.; Wiley: New York, 1984.
(9) (a) Woodward, R. B.; Hoffman, R. *The Conservation of Orbital Symmetry*; Verlag Chemie GMSH: Weinheim, 1971. (b) Eckell, A.; Huisgen, R.; Sustmann, R.; Wallbillich, G.; Grashey, D.; Spindler, E. *Chem. Ber.* **1967**, *100*, 2192.
(10) (a) Sustmann, R. *Tetrahedron Lett.* **1971**, *29*, 2717. (b) Sustmann, R. *Pure Appl. Chem.* **1974**, *40*, 569. (c) Houk, K. N.; Sims, J.; Duke, R. E., Jr.; Strozier, R. W.; George, K. *J. Am. Chem. Soc.* **1973**, *95*, 7287. (d) Houk, K. N.; Sims, J.; Watts, C. R.; Luskus, L. J. *J. Am. Chem. Soc.* **1973**, *95*, 7301.
(11) (a) Zozom, J.; Gillies, C. W.; Suenram, R. D.; Lovas, F. J. *Chem. Phys. Lett.* **1987**, *140*, 64. (b) Gillies, J. Z.; Gillies, C. W.; Suenram, R. D.; Lovas, F. J. *J. Am. Chem. Soc.* **1988**, *110*, 7991.

0002-7863/91/1513-6408$02.50/0